International Journal of Nanomedicine

Dovepress
open access to scientific and medical research

Open Access Full Text Article

ORIGINAL RESEARCH

Long-term intravenous administration of carboxylated single-walled carbon nanotubes induces persistent accumulation in the lungs and pulmonary fibrosis via the nuclear factor-kappa B pathway

This article was published in the following Dove Press journal:
International Journal of Nanomedicine
30 December 2016
Number of times this article has been viewed

Yue Qin[1,*]
Suning Li[2,*]
Gan Zhao[2,*]
Xuanhao Fu[1]
Xueping Xie[1]
Yiyi Huang[1]
Xiaojing Cheng[3]
Jinbin Wei[1]
Huagang Liu[1]
Zefeng Lai[1]

[1]Pharmaceutical College, Guangxi Medical University, [2]Department of Pharmacy, The Maternal and Child Health Hospital of Guangxi Zhuang Autonomous Region, [3]Life Sciences Institute, Guangxi Medical University, Nanning, Guangxi, People's Republic of China

*These authors contributed equally to this work

Abstract: Numerous studies have demonstrated promising application of single-walled carbon nanotubes (SWNTs) in drug delivery, diagnosis, and targeted therapy. However, the adverse health effects resulting from intravenous injection of SWNTs are not completely understood. Studies have shown that levels of "pristine" or carboxylated carbon nanotubes are very high in mouse lungs after intravenous injection. We hypothesized that long-term and repeated intravenous administration of carboxylated SWNTs (c-SWNTs) can result in persistent accumulation and induce histopathologic changes in rat lungs. Here, c-SWNTs were administered repeatedly to rats via tail-vein injection for 90 days. Long-term intravenous injection of c-SWNTs caused sustained embolization in lung capillaries and granuloma formation. It also induced a persistent inflammatory response that was regulated by the nuclear factor-kappa B signaling pathway, and which resulted in pulmonary fibrogenesis. c-SWNTs trapped within lung capillaries traversed capillary walls and injured alveolar epithelial cells, thereby stimulating production of pro-inflammatory cytokines (tumor necrosis factor-alpha and interleukin-1 beta) and pro-fibrotic growth factors (transforming growth factor-beta 1). Protein levels of type-I and type-III collagens, matrix metalloproteinase-2, and the tissue inhibitor of metalloproteinase-2 were upregulated after intravenous exposure to c-SWNTs as determined by immunohistochemical assays and Western blotting, which suggested collagen deposition and remodeling of the extracellular matrix. These data suggest that chronic and cumulative toxicity of nanomaterials to organs with abundant capillaries should be assessed if such nanomaterials are applied via intravenous administration.

Keywords: lung fibrosis, carbon nanotubes, capillary embolization, inflammation, NF-κB

Introduction

"Carbon nanotubes" (CNTs) are outstanding nanomaterials due to their unique mechanical, optical, thermal, and electrical properties, which enable wide use in several areas.[1,2] Moreover, they can be modified or functionalized readily by covalent or non-covalent attachments. CNTs are promising candidates for biomedical applications, such as delivery of therapeutic agents,[3,4] diagnosis using near-infrared imaging, and photothermal treatment.[5,6] Commercial products made from CNTs are now part of daily life, and global production of CNTs has increased at least tenfold since 2006 to >4.5 kilotons per year.[7] Large-scale production and research interest in CNTs have raised concerns about their potential adverse effects on human health and

Correspondence: Zefeng Lai; Huagang Liu
Pharmaceutical College, Guangxi Medical University, 22 Shuangyong Road, Nanning 530021, Guangxi, People's Republic of China
Tel +86 771 535 0441
Fax +86 771 535 8272
Email laizefeng@foxmail.com; 46669073@qq.com

submit your manuscript | www.dovepress.com
Dovepress
http://dx.doi.org/10.2147/IJN.S123839

the environment. Having fibrous shapes and biopersistence (ie, the ability of a fiber to remain in the lungs) similar to those of asbestos fibers, CNTs have been suggested to pose an asbestos-like respiratory hazard. Also, numerous related studies have been undertaken during the past decade. Intratracheal instillation, pharyngeal aspiration, or inhalation of CNTs in the lungs of rodent models has been shown to result in oxidative stress,[8,9] inflammatory responses,[10,11] granuloma formation,[11,12] and pulmonary fibrosis.[13–15] The underlying cellular and molecular mechanisms of CNT-induced pulmonary fibrosis seem to be complicated, but some have been uncovered. CNTs can induce fibroblast-to-myofibroblast differentiation by stimulation of reactive oxygen species (ROS) production and activation of nuclear factor-kappa B (NF-κB) signaling.[16] The transforming growth factor-beta (TGF-β) signaling cascade has been elaborated to be involved in CNT-induced pulmonary inflammation, epithelial-to-mesenchymal transition (EMT), and fibrogenesis.[17–21]

Biomedical applications such as delivery of therapeutic agents and imaging diagnosis based on CNTs are carried out mainly via intravenous or subcutaneous routes. Hence, the biocompatibility and safety of CNTs introduced directly into the bloodstream or other biologic tissue should be assessed.

Non-covalently and covalently pegylated single-walled carbon nanotubes (SWNTs) have been shown to persist in the liver and spleen of mice for 4 months without apparent toxicity after single intravenous injection.[22] However, it has been observed that SWNTs dispersed in Tween® 80 aqueous solution remained in mice for 3 months after single intravenous exposure and induced low toxicity (eg, serum biochemical changes and slight pulmonary inflammation).[23] Another study suggested that multi-walled carbon nanotubes (MWNTs) injected via the intravenous route could cause mitochondrial destruction, spotty necrosis, and infiltration of inflammatory cells in the mouse liver.[24] Furthermore, intravenous exposure to high doses of CNTs might cause reproductive toxicity and embryotoxicity.[25,26] These controversial results are suggested to be associated with varied physicochemical properties of CNTs and exposure doses and time that may influence their toxicity profile. For example, metallic SWNTs induced more ROS generation than semiconducting SWNTs in several kinds of cells in vitro,[27,28] and oxidized SWNTs caused a higher percentage of early miscarriages and fetal malformations than pristine SWNTs in female mice.[29] Therefore, the potential toxicity and adverse health effects resulting from exposures to CNTs as drug-delivery systems or diagnostic agents merit further investigation.

Studies have shown increased numbers of "pristine" or carboxylated CNTs in the lungs induced slight inflammation responses after intravenous injection in mice.[23,30,31] Functionalization of SWNTs (eg, pegylation) can promote faster clearance from the reticuloendothelial system and reduce toxicity in vivo.[31,32] However, chemical molecules/groups on the surface of functionalized SWNTs can be biodegraded by neutrophils and the liver in mice, leaving partially functionalized (eg, carboxylated) or pristine SWNTs.[33,34] As candidate drug-delivery vehicles, functionalized SWNTs might be administered repeatedly to the blood circulation system for several weeks (or even several months). However, the health risks resulting from long-term intravenous injection of SWNTs are not known.

Here, we demonstrated that long-term and repeated intravenous administration of carboxylated SWNTs (c-SWNTs) for ≤90 days resulted in accumulation of c-SWNTs in the lungs and induced persistent inflammatory immune responses regulated by the NF-κB signal pathway in rats. These phenomena promoted fibrogenesis-related protein expression and the pathologic changes of lung fibrosis. Many studies have demonstrated that exposure of the respiratory tract to CNTs can lead to fibrosis. However, we provide, for the first time, evidence for pulmonary fibrosis induced by intravenous administration of c-SWNTs.

Materials and methods

Preparation of short c-SWNTs

Purified c-SWNTs (individual length, 1–3 μm; carboxyl content, 2.73 wt%) were purchased from Chengdu Organic Chemicals (Chengdu, People's Republic of China). These c-SWNTs were oxidized using mixed concentrated acid (to remove the remaining metal impurities and improve their dispersity in water) followed by length reduction (by ultrasonication). Typically, 100.0 mg of purchased c-SWNTs was mixed with 60.00 mL of 98 wt% H_2SO_4 solution and 20.00 mL of 65 wt% HNO_3 solution and stirred with a magnetic stirrer for 3 h at 65°C. The suspension obtained was neutralized with NaOH solution and cut using an ultrasonic processor (JY92-IIDN; Scientz, Beijing, People's Republic of China) for 1 h. Ions of impurities were removed by repeated filtration through a 100-kDa molecular weight cutoff filter (Merck Millipore, Billerica, MA, USA) and washing with distilled water, which yielded a concentrated aqueous solution of short c-SWNTs. The concentrated c-SWNTs solution prepared was sterilized by irradiation with ^{60}Co gamma rays and used as a stock solution. Immediately before injection, the stock solution was diluted with a medical-grade 5.00 wt%

glucose solution to required concentration and sonicated for ≥5 min in an ultrasonic bath, followed by centrifugation at 4,900× *g* for 10 min to remove potential aggregates. The concentration of c-SWNTs was determined using a Lambda 650 ultraviolet–visible spectrometer (PerkinElmer, Waltham, MA, USA) at 253 nm with a weight concentration-based extinction coefficient of 61.82 $L \cdot g^{-1} \cdot cm^{-1}$.

Characterization of c-SWNTs

The particle morphology and size of prepared c-SWNTs were determined by transmission electron microscopy (TEM) using a transmission electron microscope (H7500; Hitachi, Tokyo, Japan). Raman spectroscopy with a 785 nm laser (LS-785 Raman spectrometer; Princeton Instruments, Acton, MA, USA) was applied to characterize the structure of c-SWNTs. And the zeta potential of the c-SWNTs dispersed in 5.00 wt% glucose solution was measured using a Zetasizer Nano ZS (Malvern Instruments, Malvern, UK). The content of metal impurities was measured by inductively coupled plasma-mass spectrometry (ICP-MS) using an Elemental X7 system (Thermo Fisher Scientific, Waltham, MA, USA).

Animals, treatment, and experimental design

The care and treatment of the animals were in accordance with the guidelines established by the Ministry of Science and Technology of China on the Humane Care and Use of Laboratory Animals and were approved by the Institutional Animal Care and Use Committee of Guangxi Medical University (Guangxi, People's Republic of China; approval no 201310009).

Ninety-six specific pathogen-free Sprague Dawley rats of either sex (8 weeks; 200–250 g) were obtained from the Experimental Animal Center of Guangxi Medical University. They were housed in plastic cages and maintained under controlled temperature (22°C), relative humidity (55%±5%), and a 12-h light–dark cycle. They received water that had undergone ultrafiltration and pelleted food ab libitum.

After acclimatization to their surroundings for 1 week, rats were divided randomly into two groups of 48 each: control and c-SWNTs. They were weighed before injection. Those in the c-SWNTs group were administered c-SWNTs glucose solution (2.0 mg of c-SWNTs/kg body weight), whereas those in the control groups received 5.00 wt% glucose solution (1 mL/kg body weight), both by tail-vein injection per day. Six time periods (1, 7, 30, 60, 90, and 120 days) were set, and the rats in the "1-day" group were injected once and those in the "120-day" group were referred to 90-day injections followed by 30-day withdrawal of injections. At the end of each period, eight rats (four males and four females) were selected randomly from each group and killed after anesthesia (pentobarbital sodium, intraperitoneal injection). The lungs, livers, and kidneys were photographed, dissected, and washed with cold physiologic (0.9%) saline (toxicity data on livers and kidneys will be published in the future). One part of the lung sample was stored immediately at −80°C for analyses by Western blotting (1, 7, and 30 days) and an enzyme-linked immunosorbent assay (ELISA; 30, 60, 90, and 120 days). The remaining portion was collected for TEM observation (30 days) and histopathologic and immunohistochemical (IHC) analyses (30, 60, 90, and 120 days).

Histopathologic analyses

Fresh lung tissues were fixed in 10% phosphate-buffered formalin for 24–72 h, followed by dehydration, embedding in paraffin, cutting into slices (thickness, 5 μm), and routine staining (hematoxylin and eosin, H&E). Sections were examined to detect morphologic changes under a light microscope (CX41; Olympus, Tokyo, Japan) at 100× and 400× magnifications by a pathologist blinded to the experimental protocol.

TEM of lung tissues

To examine ultrastructural changes in lung tissues, fresh lungs of the rats in 30-day group were cut into small pieces, fixed with 2.5% glutaraldehyde in 0.1 M phosphate buffer, post-fixed with 1% osmium tetroxide, dehydrated, and resin-embedded using an embedding apparatus (ZB-J0010; Zhongxing Bairui, Beijing, People's Republic of China). Ultrathin (60 nm) sections of tissue were cut using an ultramicrotome (EM UC7; Leica, Wetzlar, Germany), collected on grids, and observed by TEM using a H7500 microscope (Hitachi) operated at 80 kV. Images were acquired with a charge-coupled device camera.

IHC analyses

Slices for IHC analyses were deparaffinized with xylene. Endogenous peroxidase was blocked with 0.3% H_2O_2 for 20 min. Sections were treated with blocking goat serum for 20 min at 37°C. Then, sections were incubated overnight at 4°C with antibodies against type-I collagen (Col I), type-III collagen (Col III), matrix metalloproteinase (MMP)-2, tissue inhibitor of metalloproteinase (TIMP)-2, TGF-β1, and alpha smooth-muscle actin (α-SMA) (1:50 dilution; Boster,

Wuhan, People's Republic of China), followed by incubation with biotin-linked secondary antibody (ZSGB-BIO, Beijing, People's Republic of China) for 10 min at 37°C and then with peroxidase-labeled streptavidin for 10 min at 37°C. Finally, sections were incubated with diaminobenzidine substrate chromogen solution (ZSGB-BIO) for 3 min and counterstained with hematoxylin. Slices were analyzed under a microscope (CX31; Olympus).

Western blotting

Liquid nitrogen was added to lung tissues, followed by homogenization to a fine powder using a mortar and pestle. After resuspension of powdered tissues, cytoplasmic extracts from lung tissues were obtained using a cytoplasmic protein extraction kit (Beyotime, Shanghai, People's Republic of China) according to manufacturer instructions. An equal amount of proteins from both groups at 1, 7, and 30 days was resolved under denaturing conditions by 8%–12% sodium dodecyl sulfate–polyacrylamide gel electrophoresis and transferred onto nitrocellulose membranes (0.22 μm). The proteins were blocked for 10 min in 5% bovine serum albumin in Tris buffered saline–Tween 20 (TBST; 25 mM Tris–HCl, pH 7.4, 125 mM sodium chloride, 0.05% Tween 20) and incubated with antibodies against Col III (1:1,000 dilution; Novus Biologicals, Littleton, CO, USA), NF-κB/p65 and inhibitor of kappa B alpha (IκBα) (1:1,000 dilution; Cell Signaling Technology, Danvers, MA, USA), tubulin (1:5,000 dilution; EarthOX Life Sciences, Millbrae, CA, USA), and glyceraldehyde 3-phosphate dehydrogenase (1:5,000 dilution; Multisciences, Hangzhou, People's Republic of China) overnight at 4°C. Membranes were washed thrice with TBST for 5 min and incubated with IRDye® 680LT goat (polyclonal) anti-rabbit (or anti-mouse) IgG (H+L) secondary antibodies (LI-COR Biosciences, Lincoln, NE, USA) for 1 h at room temperature. Images were captured using an Odyssey Infrared Imaging System v3.0.16 (LI-COR Biosciences).

Measurement of expression of pro-inflammatory cytokines

Levels of tumor necrosis factor alpha (TNFα) and interleukin-1 beta (IL-1β) in lung tissues were measured by an ELISA. ELISA kits for TNFα and IL-1β were used according to manufacturer instructions (Neobioscience, Shenzhen, People's Republic of China). The optical density was determined at 450 nm by a microplate reader (SpectraMax Plus384; Molecular Devices, Sunnyvale, CA, USA), and results are expressed as pg/mg protein. Sensitivities for TNFα and IL-1β were 11 and 30 pg/mL, respectively.

Statistical analyses

For each set of results, independent determinations were repeated at least thrice, and data are described as the mean ± standard deviation. Differences among mean values were tested by the independent *t*-test using SPSS v20.0 (IBM, Armonk, NY, USA). Comparisons were considered significant at $P<0.05$, $P<0.01$, or $P<0.001$.

Results and discussion

Physicochemical properties of c-SWNTs

Physicochemical properties (length, diameter, surface functionalization, agglomeration, dispersity, residue of metal catalysts, and structural defect) have been reported to affect CNTs toxicity and should be characterized before carrying out biologic tests.[31,35–40] Therefore, we employed a wide range of analytical methods to characterize c-SWNTs used for animal tests, and the results are shown in Figure 1.

Transmission electron micrographs revealed the outer diameters of c-SWNTs with few agglomerations ranging from 6 to 15 nm. The lengths of most nanotubes were ≤200 nm, and those of a minority were >1 μm. The ratio of Raman intensity between G band and D band (I_G/I_D) can be used to estimate the structural defects and carbonaceous impurity content of SWNTs. Here, Raman spectra measured using 785 nm excitation showed the characteristic D-band and G-band Raman peaks of SWNTs at 1,312 cm^{-1} and 1,588 cm^{-1}, respectively. And the I_G/I_D ratio of c-SWNTs was 5.50, indicating the structural defects resulting from carboxyl groups on the nanotube framework. The zeta potential of the c-SWNTs glucose solution was −44.1 mV, suggesting a high negative surface charge derived from carboxyl functionalization of nanotubes as well as provision of electrostatic repulsion that can overwhelm the van der Waals attractions between nanotubes to make them more hydrophilic. However, addition of electrolytes can produce cations that are attracted by the negative surface of carboxylated nanotubes and which can reduce aqueous dispersion of nanotubes. Consequently, to protect against coagulation of c-SWNTs, medical-grade 5.00 wt% glucose solution was employed instead of 0.9% saline solution to disperse c-SWNTs.

SWNTs were synthesized by chemical vapor deposition based on cobalt-catalyzed pyrolysis of methane and oxidized by a mixture of $KMnO_4$ and concentrated H_2SO_4 solution. Hence, residues of metal catalysts as well as other metal

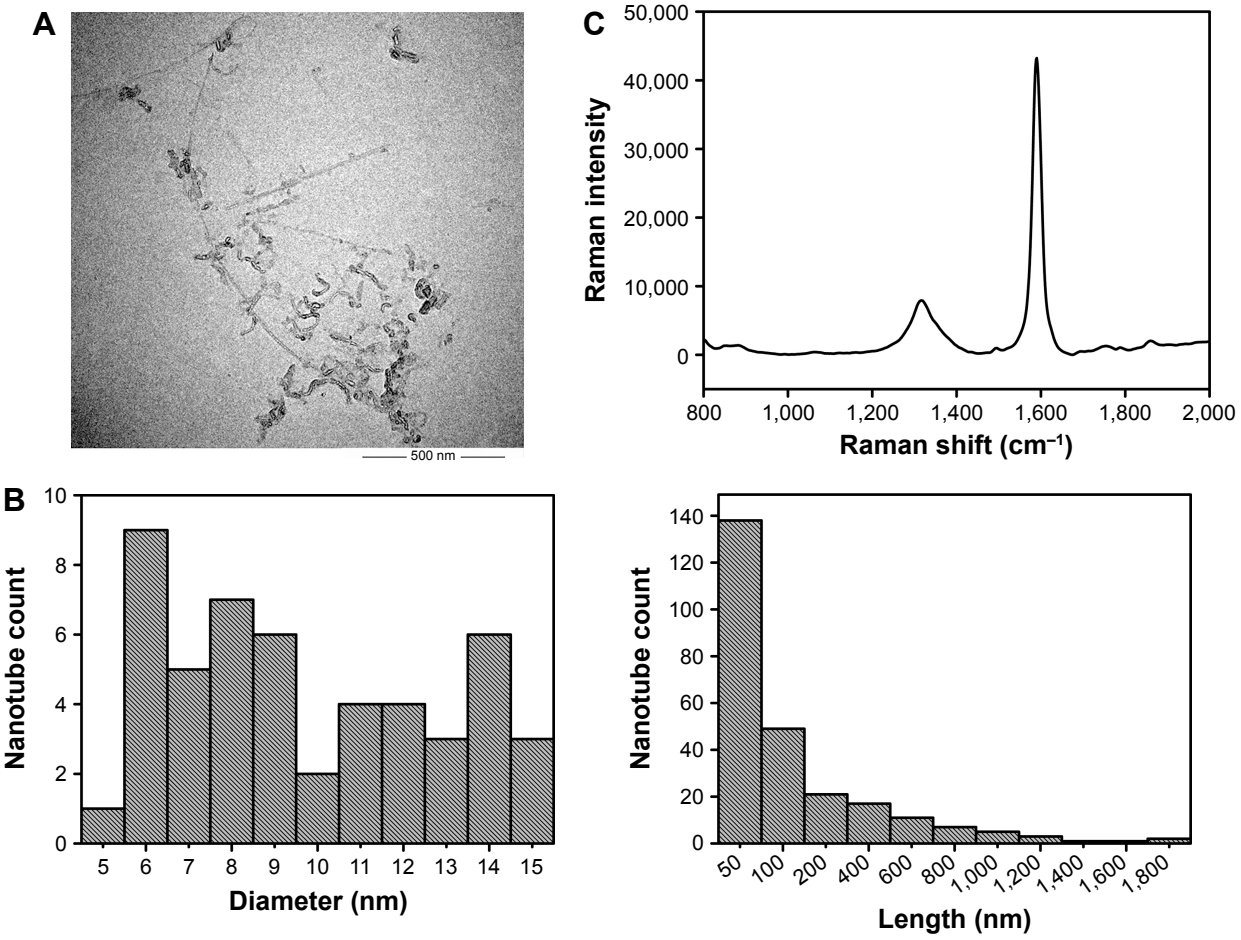

Figure 1 Characterization of c-SWNTs.
Notes: TEM image (**A**). Length and diameter distribution by TEM (**B**). Raman spectrum (**C**). I_G/I_D by Raman was 5.50. Zeta potential was −44.1 mV. Metal impurities of Al, Fe, Ti, Cr, Co, and Ni were 0.89, 0.43, 0.30, 0.08, 0.08, 0.03 wt%, respectively.
Abbreviations: TEM, transmission electron microscopy; I_G, Raman intensity of G band; I_D, Raman intensity of D band; c-SWNTs, carboxylated single-walled carbon nanotubes.

impurities could have remained in the c-SWNTs prepared. ICP-MS data suggested very low contents of various metal residues (Al, Fe, Ti, Cr, Co, Ni, Mn, and Cu) that might have been introduced from metal catalysts and the probe tip component materials of the ultrasonic processor during sonication; particularly, the contents of Mn and Cu metal residues were too low to be detected. Hence, these metal residues had no influence on toxicity assessment.

Long-term intravenous exposure to c-SWNTs induces capillary embolization, persistent inflammation, and fibrogensis in rat lungs

At necropsy, rats in the c-SWNTs group at different periods had considerable amounts of distinctive and dense SWNT aggregates (black patches) distributed uniformly throughout all lung lobes, whereas control rats had no evident morphologic changes in lung tissues (Figure 2). This appearance was different from that of SWNTs instilled within the trachea, which were distributed mainly in pulmonary bronchi or bronchioles.[12] The density of these black patches increased with increasing time, and decreased 30 days after withdrawal from injections (Figure 2B4), suggesting that chronic injection of c-SWNTs resulted in persistent accumulation and slow clearance of SWNTs in the lungs. Histopathologic examination of lung tissues stained with H&E revealed that, in general, granular aggregates of brown-black SWNTs were trapped in alveolar capillaries and perivascular interstitium (Figure 3). Pathologic changes increased progressively with administration periods: capillary embolization and angiotelectasis along with hemorrhage, degeneration and edema of the smooth muscle of blood vessels, interstitial inflammation, thickening of alveolar septa, granuloma formation;

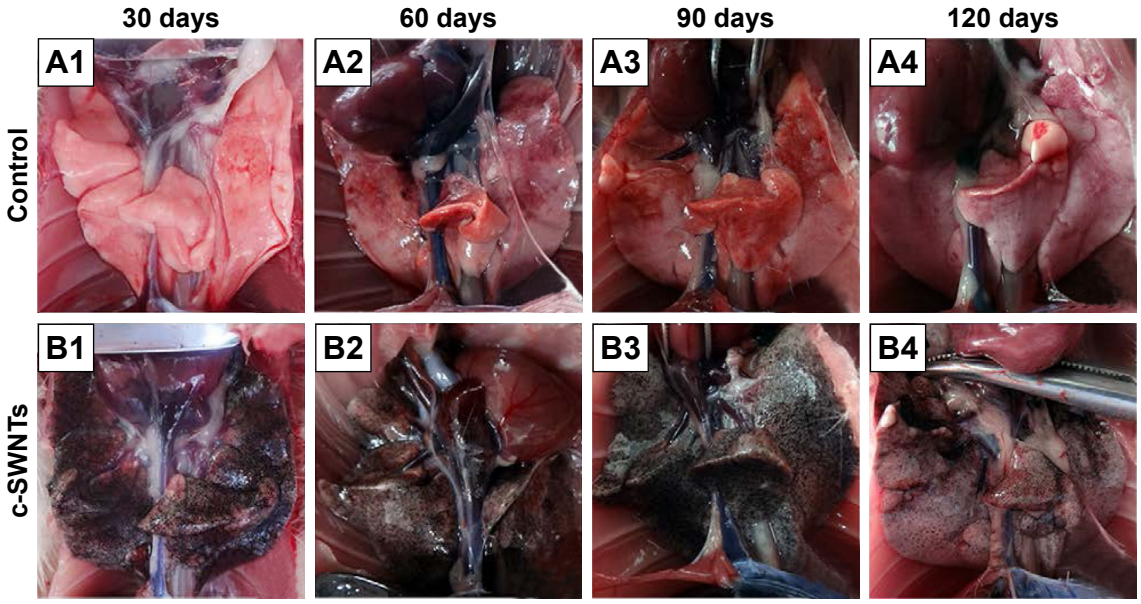

Figure 2 The dissected lungs from rats after long-term intravenous injection of c-SWNTs.
Notes: The rat lungs were dissected at the end of the setting periods (30, 60, 90, and 120 days) in the two groups: the control group (**A1**–**A4**, 5.00 wt% glucose solution, 1 mL per rat) and the c-SWNTs group (**B1**–**B4**, 2.0 mg of c-SWNTs/kg body weight per injection per rat).
Abbreviation: c-SWNTs, carboxylated single-walled carbon nanotubes.

partial destruction of alveoli structure, and deposition of collagen fibers.

Water-soluble SWNTs have been observed to "follow" oxygen-poor blood to the lungs several seconds after intravenous injection.[41] When traversing through the dense capillary network within alveolar septa, some SWNT aggregates were trapped within capillaries whose inner diameters were too small to allow only a single red blood cell to pass through. Alveolar capillaries were blocked by c-SWNT aggregates after 30-day injection (Figure 3I, B1), and the embolization in capillaries was increased at 60 and 90 days (Figure 3I, B2 and B3), respectively. However, the number of c-SWNT aggregates within capillaries decreased obviously 30 days after stopping administration (Figure 3I, B4), suggesting that capillaries could reverse c-SWNTs embolization slowly. c-SWNTs were not observed within alveolar spaces or bronchioles. This finding is in accordance with the appearance of the pulmonary lobes shown in Figure 2, but different from the situation of SWNTs instilled within the trachea, which were found in the alveoli, alveolar wall, or bronchioles of rats.[12,42] Moreover, only a few nanoparticle aggregates blocked pulmonary capillaries after a single injection.[43] At necropsy, only black patches were identified in the pulmonary lobes of rats that had received injections for >30 days (Figure 2B1), and black patches were not seen in rats that had received injections for <7 days (images not shown). Also, clearance of SWNTs given via the intravenous route was faster than that of instilled SWNTs (which were retained in rat lungs for >754 days).[12]

The embolization caused by retained c-SWNTs accumulated in alveolar capillaries led to infiltration of inflammatory cells. At 30 days, compared with one of the rats in the control group, the alveolar walls of c-SWNTs-injected rats became thicker, and the alveolar space was compressed to become narrower (Figure 3II, B1). Deposition of collagen fibers was found around the pulmonary capillaries filled with c-SWNT aggregates when the administration period was increased to 90 days (Figure 3II, B3), and was seen 30 days after stopping injections (Figure 3II, B4). These results suggest that chronic administration of SWNTs via the intravenous route may cause pulmonary fibrogenesis. It has been reported that intravenous injection of MWNTs twice per week together with consumption of a high-fat diet each day for 16 weeks causes pneumorrhagia, thickening of alveolar walls, granulomas, and fibrosis.[44] Nevertheless, the evidence of pulmonary fibrosis is not sufficient, and the related mechanism of action is not clear.

Here, we provide histopathologic evidence of pulmonary fibrosis induced by intravenous injection of c-SWNTs. At 30 days, infiltration of inflammatory cells occurred around SWNT aggregates without granuloma formation (Figure 3II, C1). When administration was prolonged to 60 days, granulomas were seen around SWNT aggregates loaded with increased numbers of inflammatory cells

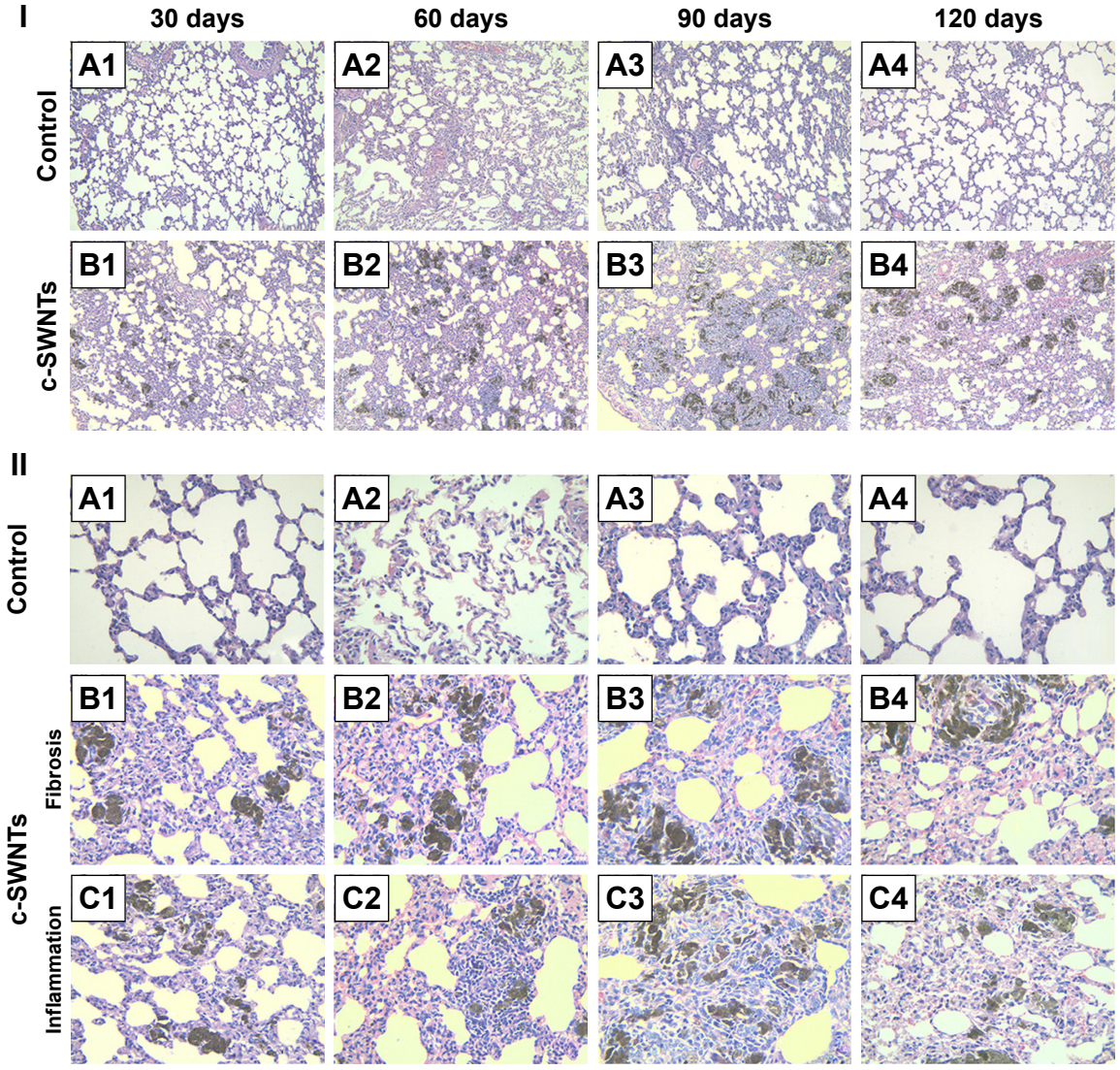

Figure 3 Long-term intravenous exposure to c-SWNTs induces capillary embolization, persistent inflammation, and fibrogensis in rat lungs.
Notes: Representative histopathology of H&E-stained lung sections from the rats at the end of the setting periods (30, 60, 90, and 120 days) after persistent intravenous injection with 5.00 wt% glucose solution (control) or 2.0 mg of c-SWNTs/kg body weight per injection (c-SWNTs). (**I**) The control group (**A1**–**A4**); The c-SWNTs group (**B1**–**B4**). Agglomerates of c-SWNTs accumulate in the pulmonary capillary lumen, leading to embolization (magnification: 100×). (**II**) No fibrosis in the control group (**A1**–**A4**); Colllagen deposition and fibrogenesis in the c-SWNTs group (**B1**–**B4**); Infiltration of inflammatory cells within the embolized capillaries, inducing granuloma formation in the c-SWNTs groups (**C1**–**C4**) (magnification: 400×).
Abbreviations: c-SWNTs, carboxylated single-walled carbon nanotubes; H&E, hematoxylin and eosin.

(Figure 3II, C2). At 90 days, granulomas were very large, and alveolar structures were destroyed (Figure 3II, C3). Stopping injections and feeding rats with a normal diet led to smaller granulomas with less dark aggregates and fewer inflammatory cells (Figure 3II, C4). However, the severity of fibrogenesis was not alleviated.

SWNTs traverse the alveolar interstitium and induce ultrastructural alterations in alveolar epithelial cells (AECs)

To clarify further the effect of c-SWNTs injected via the intravenous route on rat lungs, we employed TEM to observe ultrastructural changes in pulmonary morphologies at 30 days. The lungs of rats treated with c-SWNTs showed clear differences in the pulmonary ultrastructure compared with those of control rats (Figure 4). Generally, the number of lamellar bodies increased dramatically, and their sizes reduced (Figure 4C and D) after exposure to SWNTs. Collagen fibers (white arrows in Figure 4E) were formed and traversed within the pulmonary interstitium. Many c-SWNTs were incorporated into the alveolar interstitium and trapped within vacuoles or phagolysosomes (red arrows in Figure 4G).

Lamellar bodies are the characteristic organelles in AECs type-II (AECs-II). They can receive, store, and

secrete pulmonary surfactants (including lipids and proteins). These surfactants can lower the surface tension at the blood–air interface to prevent the lungs from collapsing at exhalation and have important roles in the immune and inflammatory responses of the lungs because they can bind to surface receptors on immune cells and modulate production of inflammatory components.[45,46] The cells shown in Figure 4 are AECs-II evident from their typical ultrastructure of lamellar bodies. Intracellular lamellar bodies increased in number and decreased in size after exposure to c-SWNTs, a finding that is similar to a report in which AECs-II were exposed to c-SWNTs[47] or gold nanoparticles[48] in vitro. The increase in the number of lamellar bodies is thought to promote surfactant production as a defense mechanism against external agents.[49]

By combining histopathologic and TEM observations, we hypothesize that c-SWNTs that could traverse capillary walls and distribute in the pulmonary interstitium were recognized by AECs-II and triggered a series of immune responses.

Long-term intravenous exposure to c-SWNTs promotes collagen deposition and extracellular matrix (ECM) remodeling by upregulation of expression of MMP-2 and TIMP-2

Histopathologic and TEM observations suggested pulmonary fibrogenesis after rats had received repeated intravenous injection of c-SWNTs for ≥30 days. To confirm this result further, we carried out IHC staining to examine expression of ECM proteins (Col I, Col III) and the level of ECM proteases MMP-2 and its inhibitor TIMP-2 in rat lungs. We also employed Western blotting to determine the protein level of Col III in the lungs of rats receiving intravenous administration of c-SWNTs for 1, 7, and 30 days. Accumulation

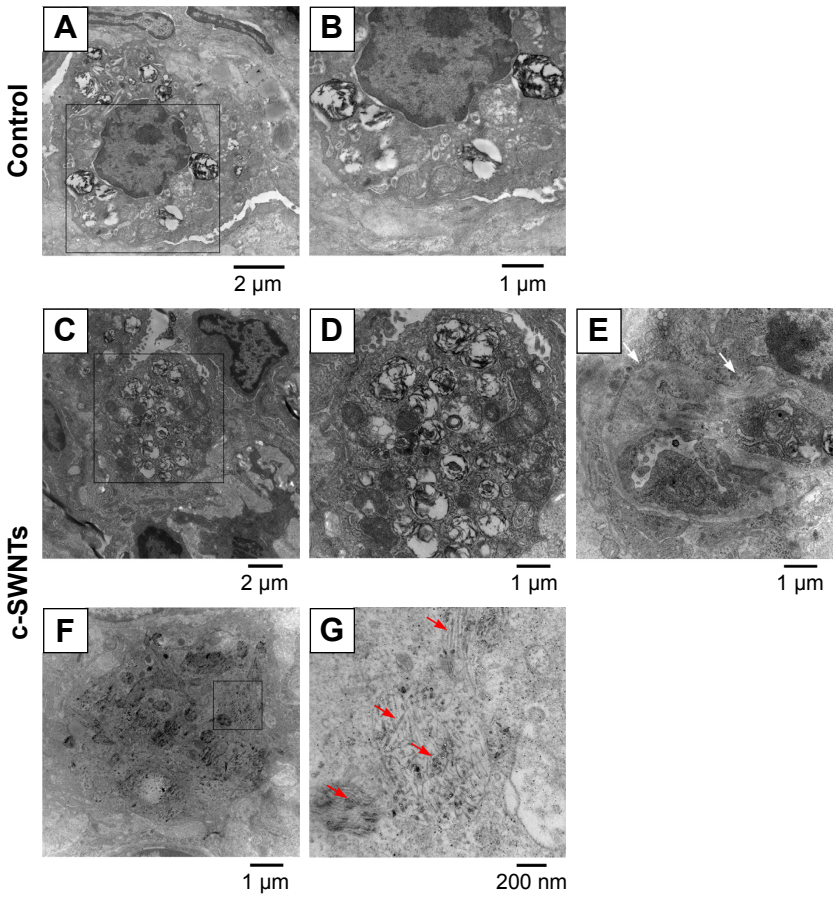

Figure 4 c-SWNTs traverse alveolar interstitium and induce ultrastructural alteration in AECs-II.
Notes: Representative TEM images of the lung sections from the rats after 30-day intravenous injection with 5.00 wt% glucose solution (control) or 2.0 mg of c-SWNTs/kg body weight per injection (c-SWNTs). Control lungs (**A**) and (**B**), wherein (**B**) is an enlarged image of the boxed region in (**A**), present normal ultrastructure of AECs-II. Exposed lungs (**C**)–(**G**), wherein (**D**) and (**G**) are enlarged images of the boxed regions in (**C**) and (**F**), respectively, show increasing lamellar bodies with decreasing sizes in AECs-II and c-SWNTs (red arrows) incorporated into the alveolar interstitium and trapped inside the vacuoles or the phagolysosomes, as well as fibril formation (**E**), (white arrows).
Abbreviations: c-SWNTs, carboxylated single-walled carbon nanotubes; AECs-II, alveolar epithelial cells type-II; TEM, transmission electron microscopy.

and remodeling of the ECM (including collagens, elastin, proteoglycans, fibronectin, laminin) has been considered to be a hallmark of fibrogenesis.[50] Col I and Col III form fibrils and are the essential components of the interstitial matrix (which makes up the bulk of the ECM).[51,52] Col I and Col III are associated closely with pulmonary fibrosis, which involves abnormal formation, degradation, and turnover of the ECM.

According to IHC staining, exposure to c-SWNTs for ≥30 days led to aberrant deposition of Col I and Col III, and was identified readily around granulomas laden with c-SWNT aggregates (Figure 5A). The synthesis of Col I and Col III was augmented sequentially with an increase in exposure time, and continued to increase 30 days after stopping administration (Figure 5B). Col III has been correlated with the "extensibility" of fibrils. To examine formation of collagen fibrils after short-term exposure to c-SWNTs, we analyzed expression of Col III at 1, 7, and 30 days by immunoblotting. Not until rats had received repeated administrations for 30 days did the level of Col III in the treatment group increase compared with that of the control group (Figure 6A). It has been reported that single intravenous injection of SWNTs to mice causes accumulation in the lungs, elevation of lung indices, and slight inflammation, but not formation of granulomas or fibrosis.[23] Based on our study, we propose that the pulmonary fibrogenesis induced by intravenous injection of SWNTs is a chronic process involving long-term and repetitive exposure that results in persistent injury to the lungs.

As discussed in this study, the central event in fibrosis is uncontrolled remodeling of the ECM, which refers to the imbalance between ECM-degrading enzymes and their endogenous inhibitors (eg, MMPs and TIMPs).[53] MMP-2 is produced by structural cells in tissue such as fibroblasts, epithelial cells, and endothelial cells. Specifically, it cleaves the basement membrane (the ECM underlying the epithelium and endothelium of parenchymal tissues).[54] Protein levels of MMP-2 and TIMP-2 are upregulated during pulmonary fibrosis and can be used to characterize fibrogenesis.[55,56]

MMP-2- and TIMP-2-positive cells (Figure 5A) were observed clearly in the lung sections of rats treated with c-SWNTs, whereas cells in the control group were almost all negative. Simultaneous upregulation of expression of MMP-2 and its antagonist TIMP-2 suggested that the pulmonary fibrosis induced by chronic exposure to SWNTs was not merely an accumulation of ECM proteins, but a dynamic condition with persistent turnover of the ECM, including increasing production and degradation of proteins. Moreover, MMP-2 is important for migration of AECs during repair after lung injury.[50] It has been demonstrated that chronic exposure of human pleural mesothelial cells to SWNTs and MWNTs in vitro for ≤4 months promotes MMP-2 expression and increases the invasion and migration of cells.[57] Hence, our data suggest that the constantly increasing level of MMP-2 derived from chronic exposure to SWNTs given via the intravenous route is responsible for the abnormal remodeling of the ECM in the lungs and the resulting fibrosis.

SWNTs stimulate production of pro-inflammatory and pro-fibrotic cytokines in rat lungs after intravenous exposure

Pulmonary fibrosis is primarily an aberrant response to persistent injury rather than a single injury to the lungs. Immune responses (including inflammation and secretion of a diverse range of cytokines) are stimulated to heal the wound. However, if a chronic inflammatory response is established, wound repair can become dysregulated, and excessive ECM accumulates at the injury site, resulting in formation of fibrotic tissue. Thus, to elucidate the pulmonary inflammation elicited by chronic exposure to SWNTs given via the intravenous route and its role in progressive fibrosis, we examined expression of pro-inflammatory and pro-fibrotic cytokines (TNFα, IL-1β, and TGF-β1) in rat lungs after such exposure.

ELISA showed levels of TNFα and IL-1β in the lung tissues of treated rats to be significantly higher than those of control rats at identical times except for the IL-1β level at 30 days (Figure 7A). TNFα and IL-1β are major pro-inflammatory cytokines strongly associated with pulmonary fibrosis. Overexpression of TNFα or IL-1β in rodent lungs can trigger spontaneous pulmonary fibrosis.[58,59] Exposure of mice to CNTs through the airways increases expression of TNFα and IL-1β at protein/mRNA levels significantly, and induces collagen deposition.[17,60] Intravenous exposure to carboxylated MWNTs also upregulates expression of TNFα and IL-1β in mouse lungs.[31] TGF-β1 is a pro-fibrotic growth factor that has a critical role in pulmonary fibrosis via stimulation of the EMT as characterized by upregulation of α-SMA expression and excessive production of ECM proteins. TNFα and IL-1β have been reported to accentuate TGF-β1-driven EMT and fibrogenesis.[61] Therefore, we analyzed expression of TGF-β1 and its induction of α-SMA by IHC analyses. We found that intravenous exposure to c-SWNTs clearly increased the numbers of

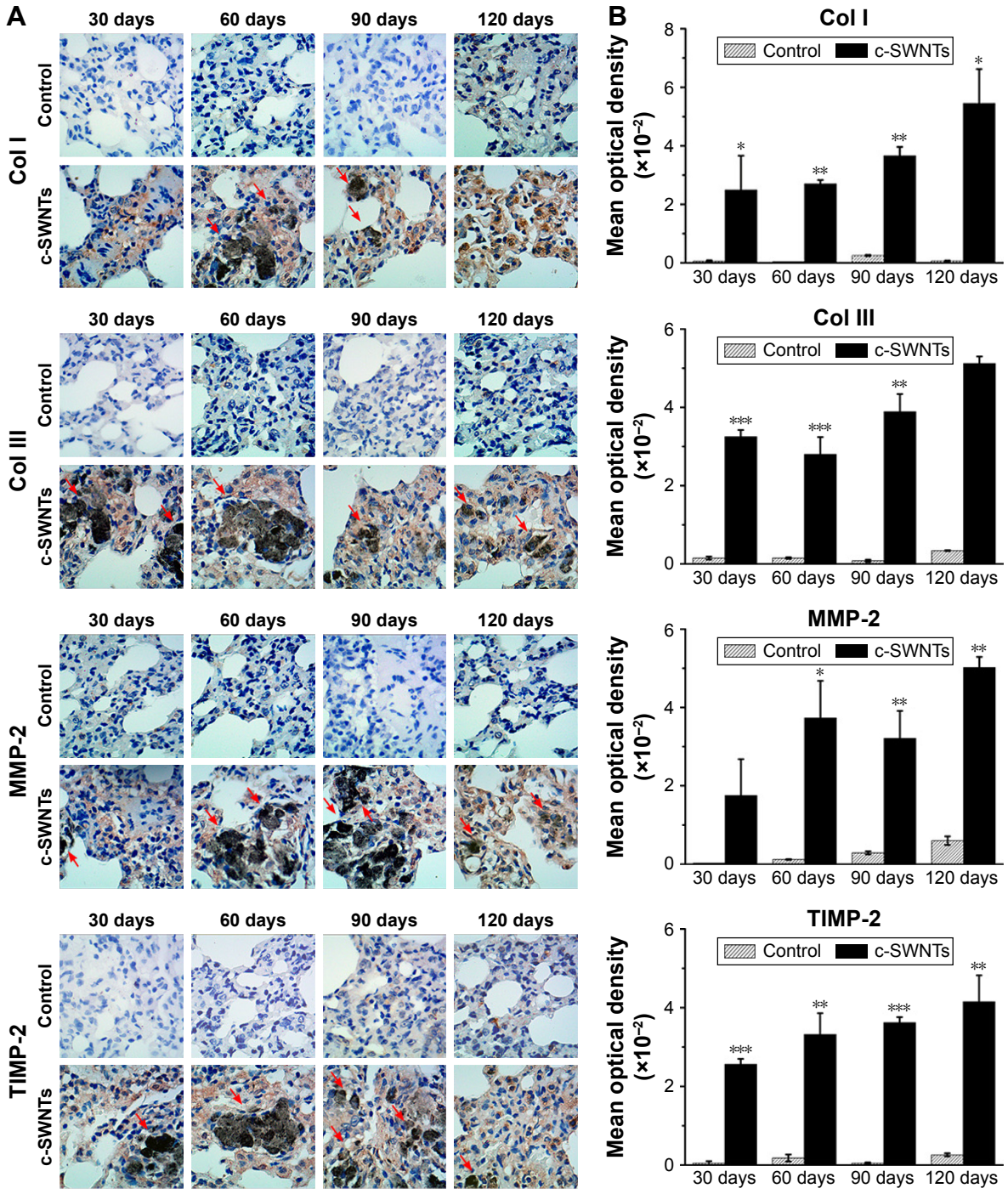

Figure 5 Long-term intravenous exposure to c-SWNTs promotes deposition of collagens and ECM remodeling by upregulating both MMP-2 and TIMP-2.

Notes: Immunohistochemical examination of Col I and Col III, MMP-2, and TIMP-2 (**A**) in the rat lungs after intravenous injection at indicated periods (positive signal: brown; c-SWNT aggregations: red arrows; magnification: 100×). Mean optical density of Col I, Col III, MMP-2, and TIMP-2 (**B**) based on immunohistochemical assay. Data represent mean ± SEM. *$P<0.05$, **$P<0.01$, and ***$P<0.001$ vs control.

Abbreviations: c-SWNTs, carboxylated single-walled carbon nanotubes; ECM, extracellular matrix; MMP-2, matrix metalloproteinase-2; TIMP-2, tissue inhibitor of metalloproteinase-2; Col I, type-I collagen; Col III, type-III collagen; SEM, standard error of the mean.

TGF-β1-positive and α-SMA-positive cells at the test periods (Figure 7B). Moreover, positive cells were distributed mainly around the brown-black SWNT aggregates. Expression of pro-inflammatory and pro-fibrotic cytokines did not decrease 30 days after stopping injections. Increased expression of TGF-β1 secreted by alveolar macrophages can stimulate mothers against decapentaplegic homolog (Smad)2 phosphorylation in rat lungs after intratracheal

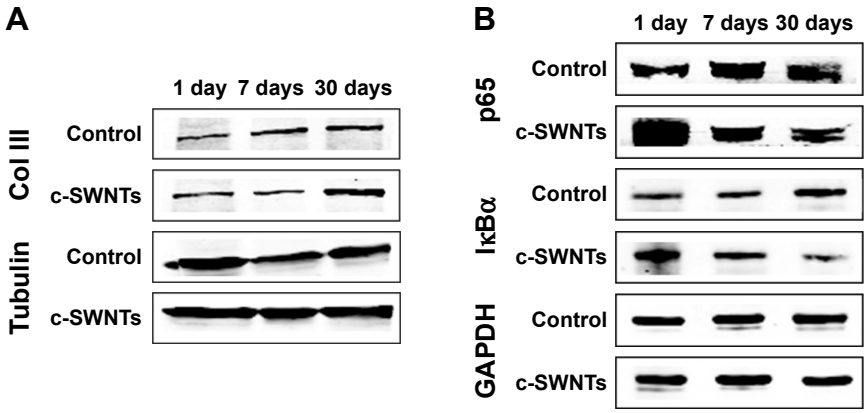

Figure 6 SWNTs stimulate the synthesis of collagen and activate NF-κB signaling in rat lungs.
Notes: Western blotting analysis of total level of Col III (**A**) and cytoplasmic levels of NF-κB/p65 and IκBα (**B**) after intravenous injection for 1, 7, and 30 days.
Abbreviations: SWNTs, single-walled carbon nanotubes; NF-κB, nuclear factor-kappa B; Col III, type-III collagen; IκBα, inhibitor of kappa B alpha; c-SWNTs, carboxylated SWNTs.

instillation of MWNTs.[18] Subsequently, the phosphorylated Smad2 heterodimerizes with Smad4 to form Smad2/4 complexes that translocate to the nucleus and bind to the promoter regions of pro-fibrotic genes such as collagen and α-SMA.[62]

Taken together, our data suggest that long-term intravenous exposure to c-SWNTs causes a persistent inflammatory response in rat lungs, which develops gradually into pulmonary fibrosis.

The inflammatory response induced by c-SWNTs is modulated through NF-κB signaling

NF-κB modulates expression of genes influencing a wide range of biologic processes: inflammation, stress responses, and metabolism.[63] Typically, in an unstimulated state, NF-κB/p65 proteins are bound and inhibited by IκBα proteins. Cytokines and growth factors such as TNFα, IL-1β, and TGF-β1 activate different signaling cascades that lead to successive phosphorylation, ubiquitination, and degradation of IκBα, allowing "liberated" phosphorylated p65 to translocate to the nucleus and trigger a "signal-amplification loop" for expression of inflammatory genes.[64]

To understand the role of the NF-κB signaling pathway in the inflammatory responses and fibrogenesis induced by c-SWNTs, we undertook immunoblotting to detect protein levels of IκBα and p65 in cytoplasmic extracts of lung tissues after rats had been treated with repeated intravenous injection for 1, 7, and 30 days.

Exposure to c-SWNTs decreased levels of IκBα and p65 in the cytoplasm at 7 and 30 days (Figure 6B), suggesting IκBα degradation and translocation of p65 proteins to the nucleus. Studies have demonstrated that MWNTs degrade IκBα and activate the NF-κB signaling pathway in macrophages to increase secretion of pro-inflammatory cytokines (eg, TNFα, IL-1β) and pro-fibrogenic growth factors (eg, TGF-β1, platelet-derived growth factor).[16,31] Uptake of SWNTs into macrophages also activates NF-κB and activator protein-1, leading to large-scale production of pro-inflammatory cytokines and pro-fibrogenic chemokines.[65] It has been validated that CNTs are able to promote expression of pro-inflammatory cytokines in vitro through ROS- and NF-κB-dependent pathways in human pulmonary epithelial cells and monocytes, which can be selectively inhibited by antioxidants and NF-κB inhibitor.[66,67] These cytokines and growth factors, in turn, amplify further NF-κB cascades through TGF-β-activated kinase-1 by regulation of positive feedback.[68,69] Taken together, the persistent lung inflammation, including the infiltration of inflammatory cells and the augment of pro-inflammatory cytokines, is modulated by the NF-κB signaling pathway activated after long-term intravenous administration of c-SWNTs, resulting in pulmonary fibrogenesis.

Consequently, we propose a scheme (Figure 8) for the mechanisms of pulmonary fibrosis induced by long-term intravenous exposure to c-SWNTs. Injected c-SWNTs become trapped within pulmonary capillaries, which results in persistent embolization and angiotelectasis. The c-SWNTs traversing into the alveolar interstitium induce injury and ultrastructural alterations to AECs-II and trigger the inflammatory response. By binding to corresponding membrane receptors, increased levels of TNFα, IL-1β, and TGF-β1 synchronously activate NF-κB/p65 signaling to strengthen the inflammatory response. The latter stimulates

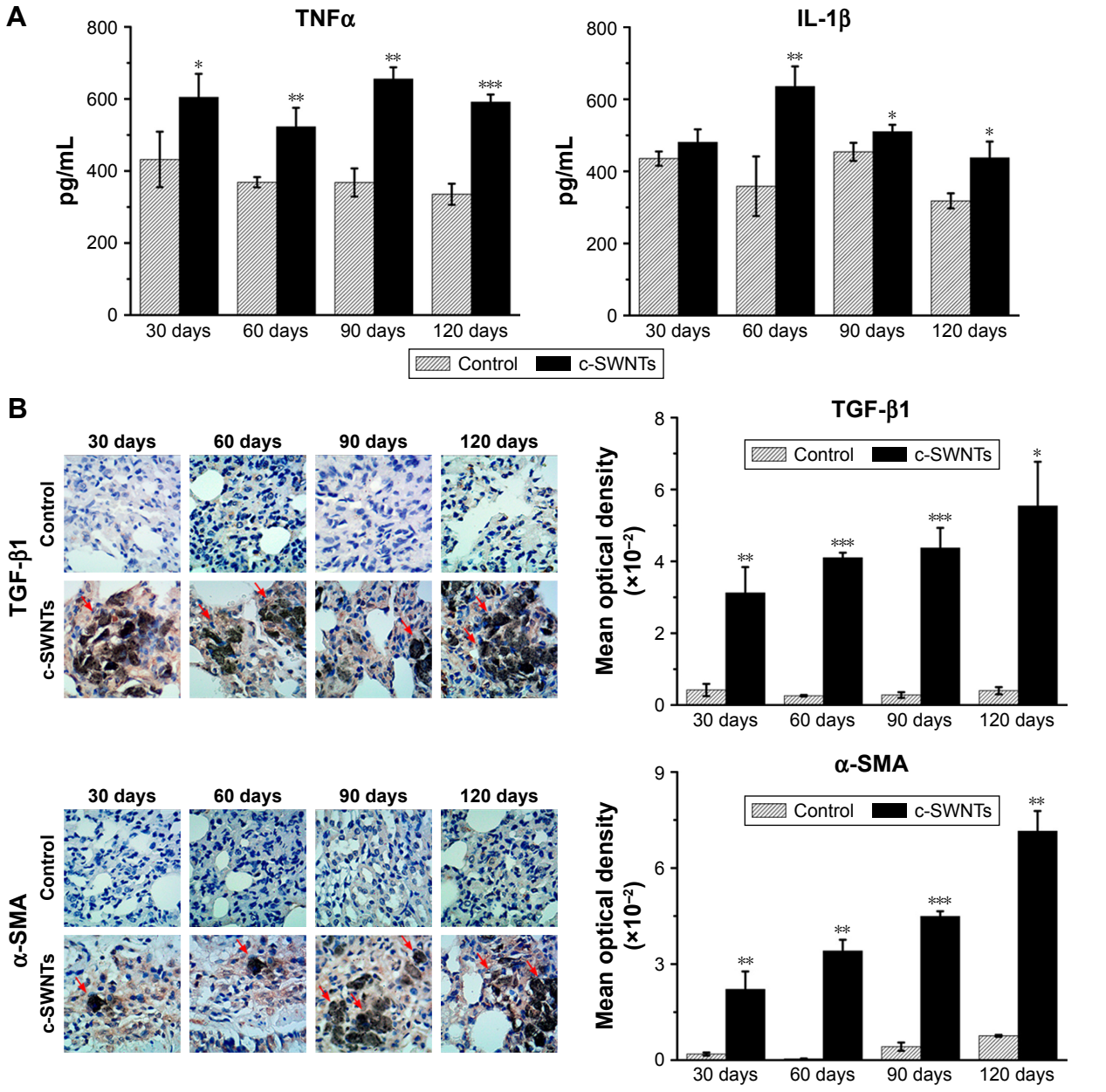

Figure 7 SWNTs stimulate production of pro-inflammatory and pro-fibrotic cytokines in rat lungs after intravenous exposure.

Notes: ELISA determination of TNFα and IL-1β levels (**A**) in the lung tissue of the rats after intravenous injection at indicated periods. Immunohistochemical examination of TGF-β1 and α-SMA, as well as the corresponding mean optical density (**B**) in the rat lungs after intravenous injection at indicated periods (positive signal: brown; c-SWNT aggregations: red arrows; magnification: 100×). Data represent mean ± SEM. *$P<0.05$, **$P<0.01$, and ***$P<0.001$ vs control.

Abbreviations: SWNTs, single-walled carbon nanotubes; ELISA, enzyme-linked immunosorbent assay; TNFα, tumor necrosis factor alpha; IL-1β, interleukin-1 beta; TGF-β1, transforming growth factor-beta 1; α-SMA, alpha smooth muscle actin; c-SWNTs, carboxylated SWNTs; SEM, standard error of the mean.

EMT of AECs-II, thereby promoting collagen synthesis and ECM deposition.

Conclusion

Long-term and repeated administration of c-SWNTs to rats via tail-vein injection caused sustained embolization in lung capillaries and induced pulmonary fibrosis resulting from chronic inflammation regulated by the NF-κB signaling pathway. Persistent injury to AECs by trapped c-SWNTs was responsible for an upregulation in expression of pro-inflammatory cytokines and pro-fibrotic growth factors. TGF-β1 had important roles in modulation of NF-κB signaling and fibrogenesis. Nevertheless, further investigations are required to elucidate the cross talk between NF-κB signaling and TGF-β signaling during regulation of CNT-induced inflammation and fibrosis.

CNTs are promising nanomaterial candidates applied in drug delivery, diagnosis, and targeted therapy. Our findings

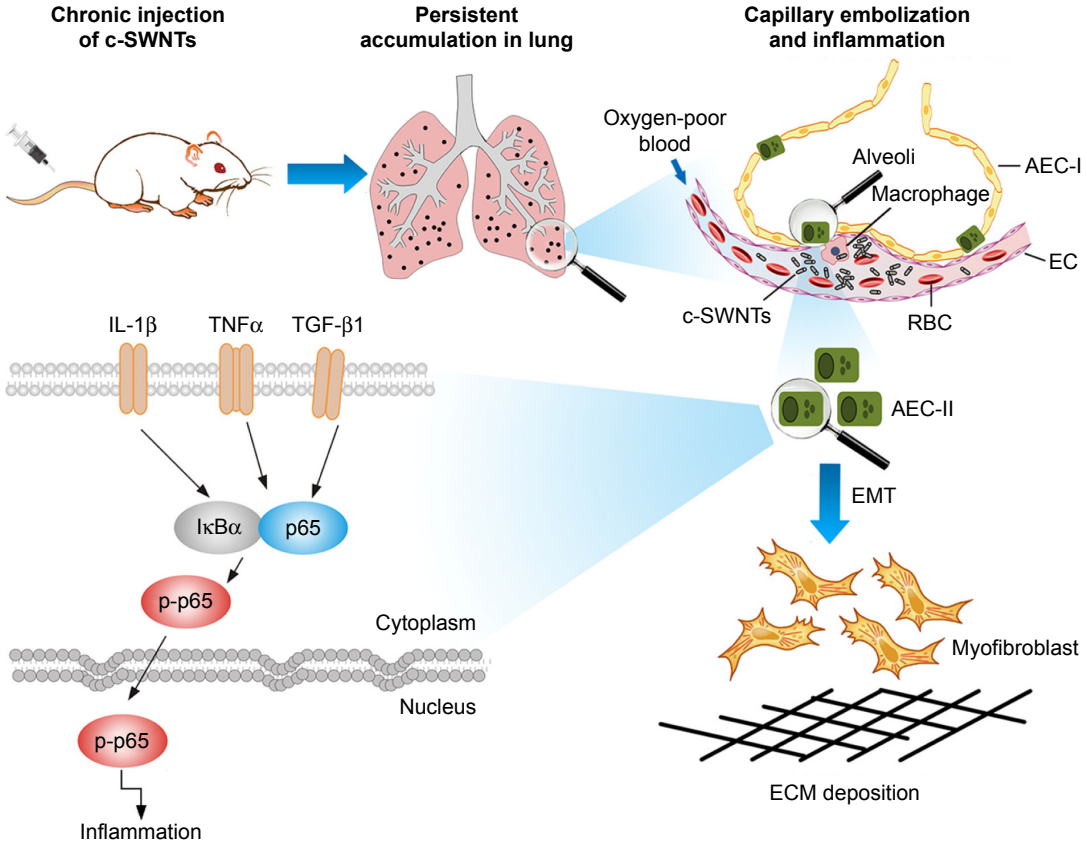

Figure 8 Schematic representation of mechanisms of pulmonary fibrosis induced by long-term intravenous exposure to c-SWNTs.
Notes: Long-term intravenous injection induces persistent accumulation of c-SWNTs in rat lung, embolization in alveolar capillary, and inflammation regulated by NF-κB pathway, resulting in EMT of AECs-II and ECM deposition.
Abbreviations: c-SWNTs, carboxylated single-walled carbon nanotubes; NF-κB, nuclear factor-kappa B; EMT, epithelial-to-mesenchymal transition; AEC-II, alveolar epithelial cell type-II; ECM, extracellular matrix; AEC-I, alveolar epithelial cell type-I; RBC, red blood cell; EC, endothelial cell; IL-1β, interleukin-1 beta; TNFα, tumor necrosis factor alpha; TGF-β1, transforming growth factor-beta 1; IκBα, inhibitor of kappa B alpha; p-p65, phosphorylated p65.

suggest that the chronic and cumulative toxicity of nanoparticles to organs with abundant capillaries should be assessed if such nanoparticles are to be applied by intravenous administration.

Acknowledgments

The authors acknowledge Professor Dr Gang Chen (Department of Pathology, First Affiliated Hospital, Guangxi Medical University) for help with histopathologic analyses. This work was supported by the National Natural Science Foundation of China (21367006).

Disclosure

The authors report no conflicts of interest in this work.

References

1. Dai L, Chang DW, Baek JB, Lu W. Carbon nanomaterials for advanced energy conversion and storage. *Small*. 2012;8(8):1130–1166.
2. Franklin AD, Luisier M, Han SJ, et al. Sub-10 nm carbon nanotube transistor. *Nano Lett*. 2012;12(2):758–762.
3. Lin L, Liu L, Zhao B, et al. Carbon nanotube-assisted optical activation of TGF-β signalling by near-infrared light. *Nat Nanotechnol*. 2015; 10(5):465–471.
4. Wong BS, Yoong SL, Jagusiak A, et al. Carbon nanotubes for delivery of small molecule drugs. *Adv Drug Deliv Rev*. 2013;65(15):1964–2015.
5. Hong G, Diao S, Chang J, et al. Through-skull fluorescence imaging of the brain in a new near-infrared window. *Nat Photon*. 2014;8(9):723–730.
6. Liang C, Diao S, Wang C, et al. Tumor metastasis inhibition by imaging-guided photothermal therapy with single-walled carbon nanotubes. *Adv Mater*. 2014;26(32):5646–5652.
7. De Volder MF, Tawfick SH, Baughman RH, Hart AJ. Carbon nanotubes: present and future commercial applications. *Science*. 2013;339(6119): 535–539.
8. Lin Z, Ma L, X ZG, Zhang H, Lin B. A comparative study of lung toxicity in rats induced by three types of nanomaterials. *Nanoscale Res Lett*. 2013;8(1):521.
9. Tabet L, Bussy C, Setyan A, et al. Coating carbon nanotubes with a polystyrene-based polymer protects against pulmonary toxicity. *Part Fibre Toxicol*. 2011;8:3.
10. Pothmann D, Simar S, Schuler D, et al. Lung inflammation and lack of genotoxicity in the comet and micronucleus assays of industrial multi-walled carbon nanotubes Graphistrength® C100 after a 90-day nose-only inhalation exposure of rats. *Part Fibre Toxicol*. 2015;12:21.
11. Warheit DB, Laurence BR, Reed KL, Roach DH, Reynolds GA, Webb TR. Comparative pulmonary toxicity assessment of single-wall carbon nanotubes in rats. *Toxicol Sci*. 2004;77(1):117–125.
12. Fujita K, Fukuda M, Fukui H, et al. Intratracheal instillation of single-wall carbon nanotubes in the rat lung induces time-dependent changes in gene expression. *Nanotoxicology*. 2015;9(3):290–301.
13. Manke A, Luanpitpong S, Dong C, et al. Effect of fiber length on carbon nanotube-induced fibrogenesis. *Int J Mol Sci*. 2014;15(5):7444–7461.

14. Porter DW, Hubbs AF, Chen BT, et al. Acute pulmonary dose-responses to inhaled multi-walled carbon nanotubes. *Nanotoxicology*. 2013;7(7):1179–1194.
15. Poulsen SS, Saber AT, Williams A, et al. MWCNTs of different physicochemical properties cause similar inflammatory responses, but differences in transcriptional and histological markers of fibrosis in mouse lungs. *Toxicol Appl Pharmacol*. 2015;284(1):16–32.
16. He X, Young SH, Schwegler-Berry D, Chisholm WP, Fernback JE, Ma Q. Multiwalled carbon nanotubes induce a fibrogenic response by stimulating reactive oxygen species production, activating NF-κB signaling, and promoting fibroblast-to-myofibroblast transformation. *Chem Res Toxicol*. 2011;24(12):2237–2248.
17. Ronzani C, Spiegelhalter C, Vonesch JL, Lebeau L, Pons F. Lung deposition and toxicological responses evoked by multi-walled carbon nanotubes dispersed in a synthetic lung surfactant in the mouse. *Arch Toxicol*. 2012;86(1):137–149.
18. Wang P, Nie X, Wang Y, et al. Multiwall carbon nanotubes mediate macrophage activation and promote pulmonary fibrosis through TGF-β/Smad signaling pathway. *Small*. 2013;9(22):3799–3811.
19. Wang X, Xia T, Ntim SA, et al. Dispersal state of multiwalled carbon nanotubes elicits profibrogenic cellular responses that correlate with fibrogenesis biomarkers and fibrosis in the murine lung. *ACS Nano*. 2011;5(12):9772–9787.
20. Chang CC, Tsai ML, Huang HC, Chen CY, Dai SX. Epithelial-mesenchymal transition contributes to SWCNT-induced pulmonary fibrosis. *Nanotoxicology*. 2012;6(6):600–610.
21. Chen T, Nie H, Gao X, et al. Epithelial-mesenchymal transition involved in pulmonary fibrosis induced by multi-walled carbon nanotubes via TGF-beta/Smad signaling pathway. *Toxicol Lett*. 2014;226(2):150–162.
22. Schipper ML, Nakayama-Ratchford N, Davis CR, et al. A pilot toxicology study of single-walled carbon nanotubes in a small sample of mice. *Nat Nanotechnol*. 2008;3(4):216–221.
23. Yang ST, Wang X, Jia G, et al. Long-term accumulation and low toxicity of single-walled carbon nanotubes in intravenously exposed mice. *Toxicol Lett*. 2008;181(3):182–189.
24. Ji Z, Zhang D, Li L, et al. The hepatotoxicity of multi-walled carbon nanotubes in mice. *Nanotechnology*. 2009;20(44):445101.
25. Bai Y, Zhang Y, Zhang J, et al. Repeated administrations of carbon nanotubes in male mice cause reversible testis damage without affecting fertility. *Nat Nanotechnol*. 2010;5(9):683–689.
26. Campagnolo L, Massimiani M, Palmieri G, et al. Biodistribution and toxicity of pegylated single wall carbon nanotubes in pregnant mice. *Part Fibre Toxicol*. 2013;10:21.
27. Wang X, Mansukhani ND, Guiney LM, et al. Toxicological profiling of highly purified metallic and semiconducting single-walled carbon nanotubes in the rodent lung and *E. coli*. *ACS Nano*. 2016;10(6):6008–6019.
28. Vecitis CD, Zodrow KR, Kang S, Elimelech M. Electronic-structure-dependent bacterial cytotoxicity of single-walled carbon nanotubes. *ACS Nano*. 2010;4(9):5471–5479.
29. Pietroiusti A, Massimiani M, Fenoglio I, et al. Low doses of pristine and oxidized single-wall carbon nanotubes affect mammalian embryonic development. *ACS Nano*. 2011;5(6):4624–4633.
30. Yang ST, Guo W, Lin Y, et al. Biodistribution of pristine single-walled carbon nanotubes in vivo. *J Phys Chem C*. 2007;111(48):17761–17764.
31. Gao N, Zhang Q, Mu Q, et al. Steering carbon nanotubes to scavenger receptor recognition by nanotube surface chemistry modification partially alleviates NFκB activation and reduces its immunotoxicity. *ACS Nano*. 2011;5(6):4581–4591.
32. Liu Z, Davis C, Cai W, He L, Chen X, Dai H. Circulation and long-term fate of functionalized, biocompatible single-walled carbon nanotubes in mice probed by Raman spectroscopy. *Proc Natl Acad Sci U S A*. 2008;105(5):1410–1415.
33. Lu N, Li J, Tian R, Peng YY. Binding of human serum albumin to single-walled carbon nanotubes activated neutrophils to increase production of hypochlorous acid, the oxidant capable of degrading nanotubes. *Chem Res Toxicol*. 2014;27(6):1070–1077.
34. Yang ST, Wang H, Meziani MJ, Liu Y, Wang X, Sun YP. Biodefunctionalization of functionalized single-walled carbon nanotubes in mice. *Biomacromolecules*. 2009;10(7):2009–2012.
35. Cheng J, Cheng SH. Influence of carbon nanotube length on toxicity to zebrafish embryos. *Int J Nanomedicine*. 2012;7:3731–3739.
36. Zhao X, Lu D, Hao F, Liu R. Exploring the diameter and surface dependent conformational changes in carbon nanotube-protein corona and the related cytotoxicity. *J Hazard Mater*. 2015;292:98–107.
37. Wang JT, Fabbro C, Venturelli E, et al. The relationship between the diameter of chemically-functionalized multi-walled carbon nanotubes and their organ biodistribution profiles in vivo. *Biomaterials*. 2014;35(35):9517–9528.
38. Wick P, Manser P, Limbach LK, et al. The degree and kind of agglomeration affect carbon nanotube cytotoxicity. *Toxicol Lett*. 2007;168(2):121–131.
39. Lee S, Khang D, Kim SH. High dispersity of carbon nanotubes diminishes immunotoxicity in spleen. *Int J Nanomedicine*. 2015;10:2697–2710.
40. Wang X, Qu R, Huang Q, Wei Z, Wang Z. Hepatic oxidative stress and catalyst metals accumulation in goldfish exposed to carbon nanotubes under different pH levels. *Aquat Toxicol*. 2015;160:142–150.
41. Welsher K, Sherlock SP, Dai H. Deep-tissue anatomical imaging of mice using carbon nanotube fluorophores in the second near-infrared window. *Proc Natl Acad Sci U S A*. 2011;108(22):8943–8948.
42. Fujita K, Fukuda M, Endoh S, et al. Size effects of single-walled carbon nanotubes on in vivo and in vitro pulmonary toxicity. *Inhal Toxicol*. 2015;27(4):207–223.
43. Wang X, Podila R, Shannahan JH, Rao AM, Brown JM. Intravenously delivered graphene nanosheets and multiwalled carbon nanotubes induce site-specific Th2 inflammatory responses via the IL-33/ST2 axis. *Int J Nanomedicine*. 2013;8:1733–1748.
44. Gu XM, Hu P, Shen T, et al. [Pulmonary toxicity in high-fat diet SD rats induced by intravenous injection of multi-walled carbon nanotubes]. *Zhonghua Lao Dong Wei Sheng Zhi Ye Bing Za Zhi*. 2012;30(6):413–417. Chinese [with English abstract].
45. Chroneos ZC, Sever-Chroneos Z, Shepherd VL. Pulmonary surfactant: an immunological perspective. *Cell Physiol Biochem*. 2010;25(1):13–26.
46. Guillot L, Nathan N, Tabary O, et al. Alveolar epithelial cells: master regulators of lung homeostasis. *Int J Biochem Cell Biol*. 2013;45(11):2568–2573.
47. Ruge CA, Schaefer UF, Herrmann J, et al. The interplay of lung surfactant proteins and lipids assimilates the macrophage clearance of nanoparticles. *PLoS One*. 2012;7(7):e40775.
48. Wang M, Petersen NO. Lipid-coated gold nanoparticles promote lamellar body formation in A549 cells. *Biochim Biophys Acta*. 2013;1831(6):1089–1097.
49. Stringer B, Kobzik L. Alveolar macrophage uptake of the environmental particulate titanium dioxide: role of surfactant components. *Am J Respir Cell Mol Biol*. 1996;14(2):155–160.
50. Thannickal VJ, Toews GB, White ES, Lynch JP 3rd, Martinez FJ. Mechanisms of pulmonary fibrosis. *Annu Rev Med*. 2004;55:395–417.
51. Karsdal MA, Nielsen MJ, Sand JM, et al. Extracellular matrix remodeling: the common denominator in connective tissue diseases. Possibilities for evaluation and current understanding of the matrix as more than a passive architecture, but a key player in tissue failure. *Assay Drug Dev Technol*. 2013;11(2):70–92.
52. Kristensen JH, Karsdal MA, Genovese F, et al. The role of extracellular matrix quality in pulmonary fibrosis. *Respiration*. 2014;88(6):487–499.
53. Salazar LM, Herrera AM. Fibrotic response of tissue remodeling in COPD. *Lung*. 2011;189(2):101–109.
54. Corbel M, Belleguic C, Boichot E, Lagente V. Involvement of gelatinases (MMP-2 and MMP-9) in the development of airway inflammation and pulmonary fibrosis. *Cell Biol Toxicol*. 2002;18(1):51–61.
55. Hayashi T, Stetler-Stevenson WG, Fleming MV, et al. Immunohistochemical study of metalloproteinases and their tissue inhibitors in the lungs of patients with diffuse alveolar damage and idiopathic pulmonary fibrosis. *Am J Pathol*. 1996;149(4):1241–1256.

56. Kim JY, Choeng HC, Ahn C, Cho SH. Early and late changes of MMP-2 and MMP-9 in bleomycin-induced pulmonary fibrosis. *Yonsei Med J*. 2009;50(1):68–77.
57. Lohcharoenkal W, Wang L, Stueckle TA, et al. Chronic exposure to carbon nanotubes induces invasion of human mesothelial cells through matrix metalloproteinase-2. *ACS Nano*. 2013;7(9):7711–7723.
58. Miyazaki Y, Araki K, Vesin C, et al. Expression of a tumor necrosis factor-alpha transgene in murine lung causes lymphocytic and fibrosing alveolitis. A mouse model of progressive pulmonary fibrosis. *J Clin Invest*. 1995;96(1):250–259.
59. Kolb M, Margetts PJ, Anthony DC, Pitossi F, Gauldie J. Transient expression of IL-1beta induces acute lung injury and chronic repair leading to pulmonary fibrosis. *J Clin Invest*. 2001;107(12):1529–1536.
60. Kido T, Tsunoda M, Kasai T, et al. The increases in relative mRNA expressions of inflammatory cytokines and chemokines in splenic macrophages from rats exposed to multi-walled carbon nanotubes by whole-body inhalation for 13 weeks. *Inhal Toxicol*. 2014;26(12):750–758.
61. Borthwick LA, Wynn TA, Fisher AJ. Cytokine mediated tissue fibrosis. *Biochim Biophys Acta*. 2013;1832(7):1049–1060.
62. Camelo A, Dunmore R, Sleeman MA, Clarke DL. The epithelium in idiopathic pulmonary fibrosis: breaking the barrier. *Front Pharmacol*. 2014;4:173.
63. Tornatore L, Thotakura AK, Bennett J, Moretti M, Franzoso G. The nuclear factor kappa B signaling pathway: integrating metabolism with inflammation. *Trends Cell Biol*. 2012;22(11):557–566.
64. Zhou J, Ching YQ, Chng WJ. Aberrant nuclear factor-kappa B activity in acute myeloid leukemia: from molecular pathogenesis to therapeutic target. *Oncotarget*. 2015;6(8):5490–5500.
65. Chou CC, Hsiao HY, Hong QS, et al. Single-walled carbon nanotubes can induce pulmonary injury in mouse model. *Nano Lett*. 2008;8(2):437–445.
66. Ye S, Zhang H, Wang Y, Jiao F, Lin C, Zhang Q. Carboxylated single-walled carbon nanotubes induce an inflammatory response in human primary monocytes through oxidative stress and NF-κB activation. *J Nanopart Res*. 2011;13(9):4239–4252.
67. Ye SF, Wu YH, Hou ZQ, Zhang QQ. ROS and NF-kappaB are involved in upregulation of IL-8 in A549 cells exposed to multi-walled carbon nanotubes. *Biochem Biophys Res Commun*. 2009;379(2):643–648.
68. Jurida L, Soelch J, Bartkuhn M, et al. The activation of IL-1-induced enhancers depends on TAK1 kinase activity and NF-κB p65. *Cell Rep*. Epub 2015 Feb 4.
69. Zheng C, Zheng Z, Zhang Z, et al. IFIT5 positively regulates NF-κB signaling through synergizing the recruitment of IκB kinase (IKK) to TGF-β-activated kinase 1 (TAK1). *Cell Signal*. 2015;27(12):2343–2354.